Structural, Electronic and Magnetic Properties of Impurities Defected Graphene/MoS_2 Van Der Waals Heterostructure: First-principles Study

H. K. Neupane and N. P. Adhikari

Journal of Nepal Physical Society

Volume 7, Issue 2, June 2021

ISSN: 2392-473X (Print), 2738-9537 (Online)

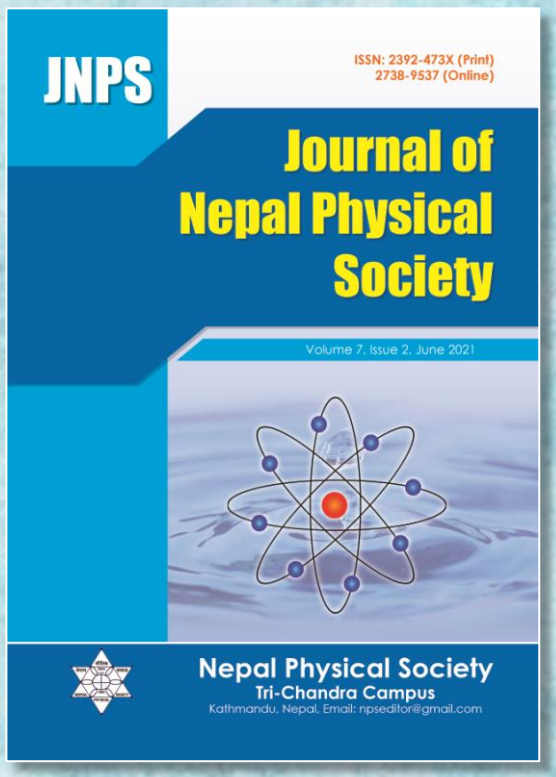

JNPS, **7** (2), 1-8 (2021)

DOI: https://doi.org/10.3126/jnphyssoc.v7i2.38578

Published by:

Nepal Physical Society

P.O. Box: 2934

Tri-Chandra Campus

Kathmandu, Nepal

Email: npseditor@gmail.com

JNPS ***7*** *(2): 1-8 (2021)*
ISSN: 2392-473X (Print), 2738-9537 (Online)

Research Article *© Nepal Physical Society*
DOI: https://doi.org/10.3126/jnphyssoc.v7i2.38578

Structural, Electronic and Magnetic Properties of Impurities Defected Graphene/MoS_2 Van Der Waals Heterostructure: First-principles Study

H. K. Neupane[1, 2] and N. P. Adhikari[2, *]
[1]Amrit Campus, Institute of Science and Technology, Tribhuvan University, Kathmandu, Nepal
[2]Central Department of Physics, Institute of Science and Technology,
Tribhuvan University, Kathmandu, Nepal
[*]Corresponding Email: narayan.adhikari@cdp.tu.edu.np

Received: *14 May, 2021;* ***Revised:*** *13 June, 2021;* ***Accepted:*** *25 June, 2021*

ABSTRACT

Two-dimensional (2D) pristine and defected van der Waals (vdW) heterostructure (HS) materials open up fortune in nanoelectronic and optoelectronic devices. So, they are compatible for designing in the fields of device applications. In the present work, we studied structural, electronic and magnetic properties of vdW (HS) graphene/MoS_2 ((HS)G/MoS_2), Nb impurity defect in vdW (HS) graphene/MoS_2 (Nb-(HS)G/MoS_2), and Tc impurity defect in vdW (HS) graphene/MoS_2 (Tc-(HS)G/MoS_2) materials by using spin-polarized DFT-D2 method. We examined the structure of these materials, and found that they are stable. Based on band structure analysis, we found that (HS)G/MoS_2, Nb-(HS)G/MoS_2 and Tc-(HS)G/MoS_2 have metallic characteristics. Also, (HS)G/MoS_2 and Tc-(HS)G/MoS_2 materials have n-type Schottky contact, while Nb-(HS)G/MoS_2 material has p-type Schottky contact. To understand the magnetic properties of materials, we have used DoS, IDoS and PDoS calculations. We found that (HS)G/MoS_2 is a non-magnetic material, but Nb-(HS)G/MoS_2 and Tc-(HS)G/MoS_2 are magnetic materials. Magnetic moment of Nb-(HS)G/MoS_2 and Tc-(HS)G/MoS_2 materials are -0.24 μ_B/cell and +0.07μ_B/cell values respectively from DoS/PDoS calculations, and 0.26 μ_B/cell and 0.08μ_B/cell values respectively from IDoS calculations. Up-spin and down-spin states of electrons in 2p orbital of C atoms, 3p orbital of S atoms, 4d orbital of Mo atoms, 4d orbital of Tc atom in Tc-(HS)G/MoS_2, and 2p orbital of C atoms, 3p orbital of S atoms, 4p & 4d orbitals of Mo atoms, 4p & 4d orbitals of Nb atom in Nb-(HS)G/MoS_2 have major contribution for the development of magnetic moment.

Keywords: DFT-D2; Heterostructure; Impurity defects; Magnetic moment; Spin states.

1. INTRODUCTION

Graphene is two dimensional (2D) stretchable, sp^2-hybridized, zero band gap and honeycomb lattice structure of carbon atoms. It has good electronic properties such as, high carrier mobility and high thermal conductivity, observable Quantum Hall effect at room temperature and existence of two dimensional gases of massless Dirac fermions [1-4]. Due to these properties, it has potential applications in the areas of nanoelectronic, optoelectronic, sensing and hydrogen storage devices [5-7]. Thus, graphene is a favorable material for the researchers to predict additional desirable properties [4, 8]. Molybdenum disulphide (MoS_2) is 2D transition metal dichalcogenide (TMD) wide band gap semiconductor of band gap 1.80 eV [9]. It can be constructed by assembling Mo and S atoms (i.e. S-Mo-S) in a triangular prismatic configuration [10]. MoS_2 has great applications in the fields of nanoelectronic and optoelectronic devices [11-14]. However, 2D materials, graphene due to zero bandgap energy, and monolayer MoS_2 due to wide gap energy have limited properties. Therefore, to tune the desirable properties in 2D materials, graphene is combined with other 2D materials and formed heterostructure

(HS). The graphene based 2D (HS) materials (G/MoS_2, G/h-BN) are used to produce novel ways for engineering electronic and optoelectronic devices [15-17]. The (HS)G/MoS_2 (heterostructure of graphene with MoS_2) offers mechanical, electronic, optical, and transport properties. Thus, it can be used in the fields of device applications [18].

Moreover, the substitution of any atom by foreign atom (impurity defect) in (HS)G/MoS_2 or removal of any atom (vacancy defect) from (HS)G/MoS_2 structure is one of the promising approaches to modify and exploit unwanted properties of any constituent. The impurity of Technetium (Tc) atom or Niobium (Nb) atom in (HS)G/MoS_2 changes its electronic and magnetic properties. Defects in (HS) give peculiar properties and carry out the new materials [19-22]. Hence, defects impact the properties of (HS) materials [23]. To our knowledge, effect of impurity defects on structural, electronic and magnetic properties of vdW (HS)G/MoS_2 material have not been reported yet. Therefore, in this paper, we learned the structural, electronic and magnetic properties of vdW (HS)G/MoS_2, and effect of Nb impurity defect in vdW (HS)G/MoS_2 (Nb-(HS)G/MoS_2) material & Tc impurity defects in vdW (HS)G/MoS_2 (Tc-(HS)G/MoS_2) material by spin-polarized DFT-D2 method based on first-principles calculations. Figs. 1(a-c) illustrated pristine (HS)G/MoS_2, Nb-(HS)G/MoS_2 and Tc-(HS)G/MoS_2 materials respectively.

2. METHODS AND MATERIALS

We used spin-polarized DFT-D2 method to learn the structural, electronic and magnetic properties of (HS)G/MoS_2 and impurity defects (Nb and Tc impurity defects) in vdW (HS)G/MoS_2 using Quantum ESPRESSO (QE) computational tool [24-26]. The electronic exchange and correlation effects in the systems are treated by Generalized Gradient Approximation (GGA) using Perdew-Burke-Ernzerhof (PBE) [27]. Rappe-Rabe-Kaxiraas-Joannopoulos (RRKJ) model of ultra-soft pseudo-potentials is used to deal the chemically active valence electrons in the systems. All structures are optimized and relaxed by Broyden-Fletcher-Goldfarb-Shanno (BFGS) [28] method. At first we have prepared G/MoS_2 heterostructure material by (4×4) supercell structure of graphene and (3×3) supercell structure of monolayer MoS_2 with 4.11% lattice mismatch. To avoid the physical interactions in the stacking direction of (HS)G/MoS_2 material, we kept a vacuum distance greater than 18 Å. The Nb impurity defect in (HS)G/MoS_2 (i.e. Nb-(HS)G/MoS_2) and Tc Impurity defect in (HS)G/MoS_2 (i.e. Tc-(HS)G/MoS_2) are obtained by replacing centre Mo atom of (HS)G/MoS_2 by Nb atom and Tc atom respectively. Then, we obtained relax Nb-(HS)G/MoS_2 and Tc-(HS)G/MoS_2 structures by using BFGS method as shown in figs. 1(b-c). We performed self consistent total energy calculation after relax calculations. For this, the Brillouin-zone of (HS) is figured out in k-space using Monkhorst-Pack scheme [29] with suitable number of mesh (6×6×1) of k-points, which is determined from the convergence test. The plane-wave expansion with kinetic energy cut-off 35 Ry and charge density cut-off 350 Ry are used for wave function and charge density respectively. Kinetic energy cut-off and charge density cut-off values are calculated from convergence plot of total energy versus energy cut-off wave function. We used Marzarri-Vanderbilt [30] method of smearing for occupations and 0.001 Ry value of degauss. We have taken "david" diagonalization method with "plain" mixing mode for self consistency with 0.6 mixing factor. Also, we have taken a mesh of (6×6×1) k-points for band structure calculations (100 k-points are chosen along the high symmetric points), and meshes of (12×12×1) k-points are used for density of states (DoS) and projected density of states (PDoS) calculations.

3. RESULTS AND DISCUSSION

In this section, we discussed in details about structural, electronic and magnetic properties of pristine (HS)G/MoS_2, and Nb & Tc impurity defected (HS)G/MoS_2 materials based on spin-polarized DFT-D2 method.

3.1 Structural Analysis

We have prepared vertical stacking configuration of vdW (HS)G/MoS_2 material by keeping supercell of graphene and supercell of MoS_2. The lattice mismatch is found to be 4.11% in vdW (HS)G/MoS_2. Lattice mismatch is fixed by differing the lattice constant because there is no direct chemical bonding between the constituent layers. Stability of (HS)G/MoS_2 material is checked by its calculated binding energy. Binding energy (-0.40 eV) of it is obtained by using equation (1), [31];

$$E_b = E_{(HS)G/MoS2} - E_G - E_{MoS2} \ldots (1)$$

Where, $E_{(HS)G/MoS2}$, E_G and E_{MoS2} represent total ground state energy of (HS)G/MoS_2, supercell of

graphene and supercell of MoS_2 respectively. The obtained binding energy (-0.40 eV) of (HS)G/MoS_2 indicates that material is energetically stable at ground state because negative value of binding energy of materials implies that they are energetically stable at ground state. We have also calculated the inter-layer distance the constituents of (HS) and found 3.37 Å value. Our calculated values of binding energy and inter-layer distance are comparable with other 2D VdW heterostructure materials [32]. In addition, we have created the stable Nb-(HS)G/MoS_2 and Tc-(HS)G/MoS_2 impurity defects materials as shown in figs. 1(b-c). The binding energy of Nb-(HS)G/MoS_2 is -0.35 eV and Tc-(HS)G/MoS_2 is -0.38 eV are calculated by using equation (2), [31]; because binding energy determines the stability of materials.

$$E_b = E_{(HS\text{-}G/MoS2)i\text{-}d} - E_G - E_{(MoS2)i\text{-}d} \ldots (2)$$

Where, $E_{(HS\text{-}G/MoS2)i\text{-}d}$, $E_{(MoS2)i\text{-}d}$ & E_G represent total ground state energy of impurity (Nb atom or Tc atom) defected (HS)G/MoS_2, impurity defected monolayer MoS_2 & graphene respectively. We measured the inter-layer distances between graphene and MoS_2 in Nb-(HS)G/MoS_2 and Tc-(HS)G/MoS_2 materials, and found that they are 3.54 Å and 3.42 Å respectively, which are comparable to other 2D heteostructure materials of values 3.31 Å and 3.19 Å [32]. Thus, the estimated binding energies and inter-layer distances of impurity defected materials are also comparable with other vdW heterostructure materials [32]. We can also test the stability of impurity defected materials relative to pristine material; we can calculate the defects formation energy (E_f). Defects formation energy is obtained by using the values of total energy of impurity defects in (HS)G/MoS_2 (E_{t1}), total energy of pristine (HS)G/MoS_2 (E_{t2}), energy of impurity (Nb or Tc) atom (E_1), and energy of isolated (replaced) Mo atom (E_2) by equation (3), [33];

$$E_f = (E_{t1}-E_{t2}) - (E_1-E_2) \ldots (3)$$

Defects formation energy of Nb-(HS)G/MoS_2 and Tc-(HS)G/MoS_2 materials are found to be 2.54 eV and 2.56 eV respectively. The negative value of formation energy indicates that the system is more stable than the pristine one, while positive value of formation energy implies that the system requires external energy for the formation of impurity defects in material. Also, lower value of defects formation energy means, materials can be favorable in computation work.

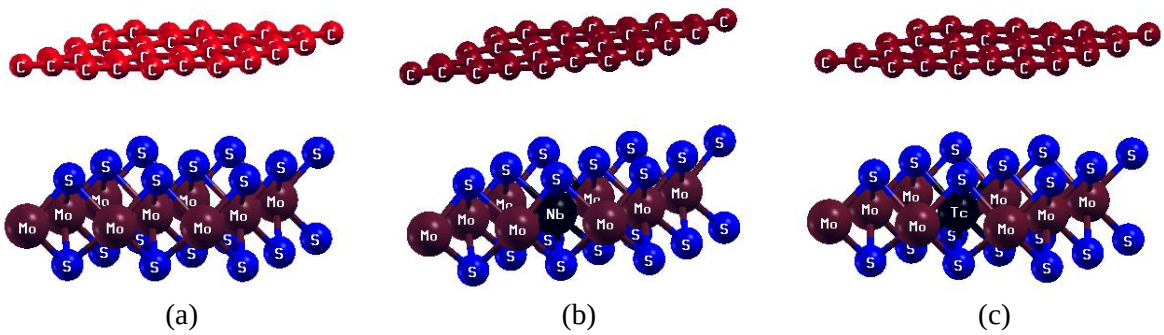

Fig. 1: (a) Structure of pristine (HS)G/MoS_2 material, (b) Structure of Nb-(HS)G/MoS_2 material, (c) Structure of Tc-(HS)G/MoS_2 material.

From the structural analysis of pristine (HS)G/MoS_2 and impurity defects Nb-(HS)G/MoS_2 & Tc-(HS)G/MoS_2 materials, we found that all are stable and compactness of pristine has greater than that of impurity defects materials.

3.2 Electronic and Magnetic Properties

Solid state matter is rigid and its degree of rigidity depends upon the relative compactness of the constituent atoms. In an isolated atom, the electrons occupy atomic orbitals each of which has a discrete energy level while atomic orbitals overlap when two identical atoms join together to form a molecule. In solid with N identical atoms, each atomic orbital splits into N discrete molecular orbitals, each with a different energy. In a macroscopic piece of solid, the number of atoms is large ($N \approx 10^{23}$), so is the number of orbitals and is very closely spaced in energy (10^{-22} eV). Thus, they

form continuum of energy as 'energy band'. Electronic properties of material can be predicted by the analysis of its band structure. In this section, we discuss electronic and magnetic properties of (HS)G/MoS_2, Nb-(HS)G/MoS_2 and Tc-(HS)G/MoS_2 materials on the basis of their band structures and density of states (DoS), integrated density of states (IDoS) and projected density of states (PDoS) analysis. The band structures of (HS)G/MoS_2, Nb-(HS)G/MoS_2 and Tc-(HS)G/MoS_2 materials are shown in fig. 2(a), fig. 3(a) and fig. 4(a) respectively. In band structures, x-axis represents Γ-centre symmetric points (Γ-M-K-Γ) in the first Brillouin-zone, where 100 k-points are kept along the particular direction of irreducible Brillouin-zone, and y-axis represents the corresponding energy values, also horizontal dotted line represents the Fermi energy level. In band structure of pristine (HS)G/MoS_2, Dirac cone is formed in the conduction band at 0.56 eV distance from Fermi energy level. It means electrons flow from valence band to conduction band. Hence, (HS)G/MoS_2 has metallic properties. Also, n-type Schottky contact is formed with Schottky barrier height of 0.42 eV in (HS)G/MoS_2. This value agrees with the reported value 0.49 eV [34, 35]. In band structures of impurity defects Nb-(HS)G/MoS_2 and Tc-(HS)G/MoS_2 materials, Dirac cone is formed in conduction band at 0.70 eV and 0.01 eV distances from the Fermi energy level as shown in fig. 3(a) and fig. 4(a) respectively. In both materials, electrons flow from valence band to conduction band, hence they have metallic properties. The n-type Schottky contact is still preserved in Tc-(HS)G/MoS_2, while in Nb-(HS)G/MoS_2 material p-type Schottky contact is formed. Therefore, n-type Schottky contact of (HS)G/MoS_2 shifts to p-type Schottky contact due to Nb impurity atom in it. We know that electronic configurations of valence electrons in Mo, Tc, Nb, S & C atoms present in the materials are [Kr] $4d^5$ $5s^1$, [Kr] $4d^5$ $5s^2$, [Kr] $4d^4$ $5s^1$, [Ne] $3s^2$ $3p^4$ & [He] $2s^2$ $2p^2$ respectively. Each Mo atom has one unpaired up-spin in 5s orbital and $4d_{xy}$, $4d_{xz}$, $4d_{yz}$, $4d_{x^2-y^2}$, $4d_{z^2}$ sub-orbitals; Tc atom has paired spins in 5s orbital and one unpaired up-spin in $4d_{xy}$, $4d_{xz}$, $4d_{yz}$, $4d_{x^2-y^2}$, $4d_{z^2}$ sub-orbitals; Nb atom has one unpaired up-spin in 5s orbital, $4d_{xy}$, $4d_{xz}$, $4d_{yz}$, $4d_{x^2-y^2}$ sub-orbitals and vacant in $4d_{z^2}$ sub-orbital; S atom has paired spins (up-spin & down-spin) in $3p_x$ sub-orbital and one unpaired up-spin in $3p_y$, $3p_z$ sub-orbitals; C atom has single up-spin in $2p_x$, $2p_y$ and vacant in $2p_z$ sub-orbitals. By the configurations of unpaired (up-spin and down-spin) spins of electrons in the orbital of atoms in (HS)G/MoS_2, Nb-(HS)G/MoS_2 and Tc-(HS)G/MoS_2 materials created different values of Fermi energy and Dirac (cone) point. The different values of Fermi energy, Dirac point, Dirac shift, Fermi shift, total energy, binding energy and inter-layer distances of above mentioned materials are given in table 1.

Table 1: Fermi energy (E_f), Fermi energy shift (E_s), Dirac (point) cone (D_p), Dirac (point) cone shift (D_s), total energy (E_t), binding energy (E_b) and inter-layer distances (D_{I-d}) of (HS)G/MoS_2, Nb-(HS)G/MoS_2 and Tc-(HS)G/MoS_2 materials.

(HS)G/MoS_2, Nb-(HS)G/MoS_2 and Tc-(HS)G/MoS_2 materials	E_f (eV)	E_s (eV)	D_p (eV)	D_s (eV)	E_t (Ry)	E_b (eV)	D_{I-d} (Å)
(HS)G/MoS_2	0.32	-	0.56	-	-2106.17	-0.40	3.37
Nb-(HS)G/MoS_2	-0.50	-0.82	0.70	+0.14	-2076.54	-0.35	3.54
Tc-(HS)G/MoS_2	0.78	+0.46	0.01	-0.55	-2138.61	-0.38	3.42

Based on DoS and PDoS calculations, we can investigate the magnetic properties of materials. Symmetrically distributed total up-spin and total down-spin in DoS/PDoS of materials means, materials has non-magnetic properties, and asymmetrically distributed unpaired up-spin and down-spin of electrons in the orbital of atom give magnetic properties of materials. The DoS and PDoS plots of (HS)G/MoS_2, Nb-(HS)G/MoS_2 and Tc-(HS)G/MoS_2 materials are given in figs 2(b-c), figs. 3(b-c) and figs. 4(b-c) respectively, where vertical dotted line distinguished energy bands (the region below zero scale is called valence band and the region above zero scale is called conduction band), and horizontal dotted line separates distributed up-spin and down-spin states of electrons in the orbitals of atoms in materials.

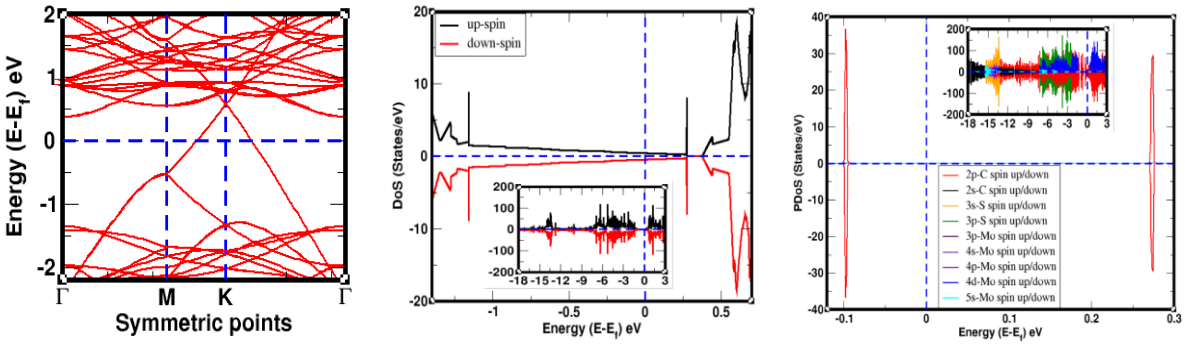

(a) (b) (c)

Fig. 2: (a) Band structure of (HS)G/MoS_2 material, (b) DoS of up-spin and down-spin states of electrons in the orbitals of C, Mo & S atoms of (HS)G/MoS_2 material (c) PDoS of individual up-spin and down-spin states of electrons in the orbitals of C, Mo & S atoms of (HS)G/MoS_2 material, where in band structure, horizontal dotted line represents Fermi level and in DoS/PDoS plots, vertical dotted line represents Fermi level. In all DoS and PDoS plots, insets represent the symmetrically distributed total up-spin and total down-spin of electrons in the orbital of atoms present in (HS)G/MoS_2 material.

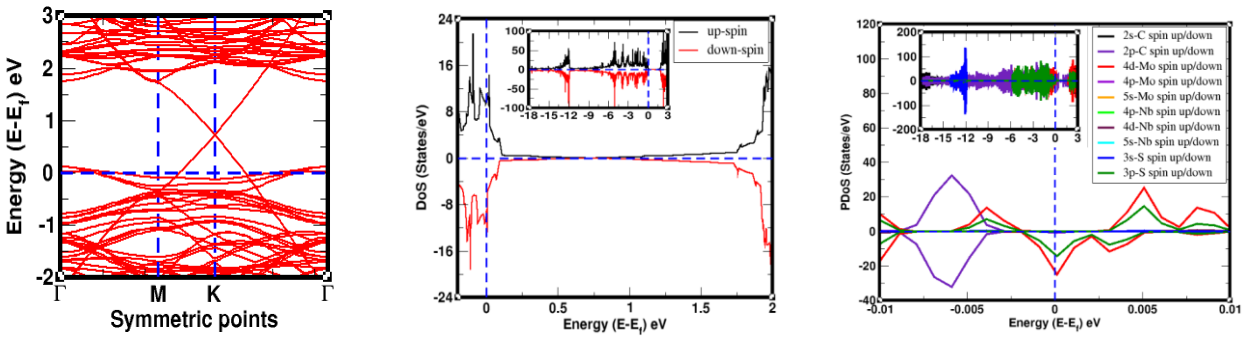

(a) (b) (c)

Fig. 3: (a) Band structure of Nb-(HS)G/MoS_2 material, (b) DoS of up-spin and down-spin states of electrons in the orbitals of C, Mo, S & Nb atoms of Nb-(HS)G/MoS_2 material (c) PDoS of individual up-spin and down-spin states of electrons in the orbitals of C, Mo, S & Nb atoms of Nb-(HS)G/MoS_2 material, where in band structure, horizontal dotted line represents Fermi level and in DoS/PDoS plots, vertical dotted line represents Fermi level. In all DoS and PDoS plots, insets represent the asymmetrically distributed total up-spin and total down-spin of electrons in the orbital of atoms present in Nb-(HS)G/MoS_2 material.

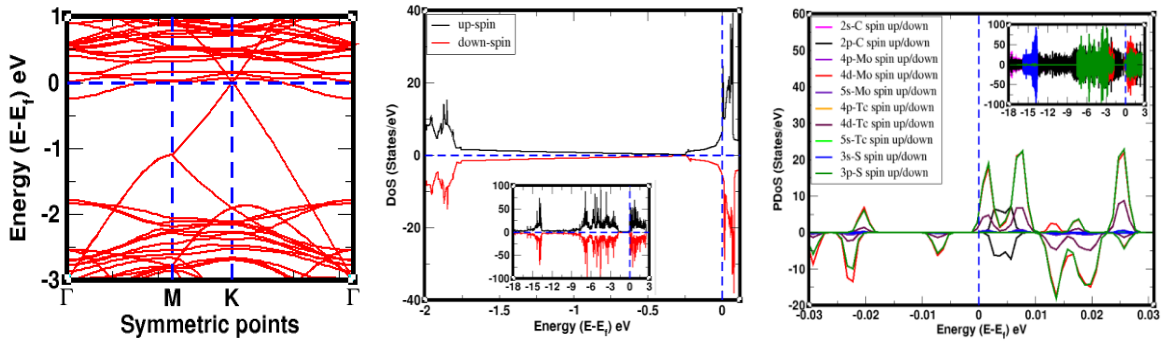

(a) (b) (c)

Fig. 4: (a) Band structure of Tc-(HS)G/MoS_2 material, (b) DoS of up-spin and down-spin states of electrons in the orbitals of C, Mo, S & Tc atoms of Tc-(HS)G/MoS_2 material (c) PDoS of individual up-spin and down-spin states of electrons in the orbitals of C, Mo, S & Tc atoms of Tc-(HS)G/MoS_2 material, where in band structure, horizontal dotted line represents Fermi level and in DoS/PDoS plots, vertical dotted line represents Fermi level. In all DoS and PDoS plots, insets represent the asymmetrically distributed total up-spin and total down-spin of electrons in the orbital of atoms present in Tc-(HS)G/MoS_2 material.

The detail calculations of magnetic moment due to spin states of electrons in the orbitals of C, Mo, S, Nb & Tc atoms in PDoS of (HS)G/MoS_2, Nb-(HS)G/MoS_2 and Tc-(HS)G/MoS_2 materials are given in table 2.

Table 2: Total magnetic moment (μ_T) of Nb-(HS)G/MoS2 and Tc-(HS)G/MoS_2 materials are obtained by asymmetrically distributed up-spin and down-spin of electrons in 2s & 2p orbitals of C atoms; 4p, 4d & 5s orbitals of Mo atoms; 3s & 3p orbitals of S atoms; 4p, 4d & 5s orbitals of Nb atoms, and 4p, 4d & 5s orbitals of Tc atoms in the materials.

Magnetic moments (μ) of (HS)G/MoS_2, Nb-(HS)G/MoS_2 and Tc-(HS)G/MoS_2 materials	Nb-(HS)G/MoS_2 (μ_B/cell)	Tc-(HS)G/MoS_2 (μ_B/cell)
μ of C atoms by distributed spins in 2s orbital	0.00	0.00
μ of C atoms by distributed spins in 2p orbital	-0.01	0.01
μ of Mo atoms by distributed spins in 4p orbital	-0.03	0.00
μ of Mo atoms by distributed spins in 4d orbital	-0.10	0.02
μ of Mo atoms by distributed spins in 5s orbital	0.00	0.00
μ of S atoms by distributed spins in 3s orbital	0.00	0.00
μ of S atoms by distributed spins in 3p orbital	-0.08	0.04
μ of Nb atom by distributed spins in 4p orbital	-0.01	-
μ of Nb atom by distributed spins in 4d orbital	-0.01	-
μ of Nb atom by distributed spins in 5s orbital	0.00	-
μ of Tc atom by distributed spins in 4p orbital	-	0.00
μ of Tc atom by distributed spins in 4d orbital	-	0.01
μ of Tc atom by distributed spins in 5s orbital	-	0.00
Total magnetic moment (μ_T) μ_B/cell	-0.24	0.07

We observed that in DoS and PDoS plots of (HS)G/MoS_2 material, up-spin and down-spin states are symmetrically distributed near the Fermi energy level as shown in figs. 2(b-c). And we obtained the value of net magnetic moment given by up-spin down-spin of electrons in all individual orbital of C, Mo, & S atoms are of zero (0.00μ_B/cell) value. We also calculated the magnetic moment due to integrated DoS and found that it is 0.00μ_B/cell. Therefore, (HS)G/MoS_2 has non-magnetic properties.

Additionally, PDoS of up-spin and down-spin states of electrons near the Fermi level of Nb-(HS)G/MoS_2 are asymmetrically distributed as shown in figs. 3(b-c). The magnetic moment developed due to the distributed up-spin and down-spin in 2s & 2p orbitals of C atoms are 0.00 μ_B/cell & -0.01μ_B/cell; 4p, 4d & 5s orbitals of Mo atoms are -0.03μ_B/cell, -0.10 μ_B/cell & -0.0oμ_B/cell; 3s & 3p orbitals of S atoms are 0.00μ_B/cell & -0.08 μ_B/cell; 4p, 4d & 5s orbitals of Nb atoms are -0.01μ_B/cell, -0.01 μ_B/cell & 0.00 μ_B/cell values respectively. We obtained the total magnetic moment of Nb-(HS)G/MoS_2 material is -0.24 μ_B/cell. Also, we have estimated the magnetic moment of Nb-(HS)G/MoS_2 material based on integrated density of states (IDoS) is 0.26 μ_B/cell. Therefore, Nb-(HS)G/MoS_2 material is called magnetic material. PDoS of up-spin and down-spin states of electrons are asymmetrically distributed around the Fermi energy level of Tc-(HS)G/MoS_2 material as shown in figs. 4(b-c). Magnetic moment developed in material due to unpaired up-spin and down-spin of electrons in 2s & 2p orbitals of C atoms are 0.00 μ_B/cell & 0.01 μ_B/cell; 4p, 4d & 5s orbitals of Mo atoms are 0.00 μ_B/cell, 0.02 μ_B/cell & 0.00 μ_B/cell; 3s & 3p orbitals of S atoms are 0.00 μ_B/cell & 0.04 μ_B/cell; 4p, 4d & 5s orbitals of Tc atoms are 0.00 μ_B/cell, 0.01 μ_B/cell & 0.00 μ_B/cell values respectively. The calculated value of total magnetic moment of Tc-(HS)G/MoS_2 material is 0.07 μ_B/cell. We calculated the magnetic moment of Tc-(HS)G/MoS_2 based on IDoS, which is 0.08 μ_B/cell value. Hence, Tc-(HS)G/MoS_2 material is also called magnetic material. Therefore, non-magnetic (HS)G/MoS_2 changes to magnetic Nb-

(HS)G/MoS_2 and Tc-(HS)G/MoS_2 materials due to Nb and Tc impurity defects respectively. In impurity defected Nb-(HS)G/MoS_2 material, major contribution of magnetic moment is given by distributed spin states in 4p, 4d orbitals of Mo atoms and 3p orbital of S atoms, while distributed spin states in 4d orbital of Mo atoms and 3p orbital of S atoms have dominant role for the development of magnetic moment in Tc-(HS)G/MoS_2 material.

4. CONCLUSIONS

Structural, electronic and magnetic properties of (HS)G/MoS_2, Nb-(HS)G/MoS_2 and Tc-(HS)G/MoS_2 materials have been studied using spin-polarized DFT with vdW corrections DFT-D2 approach. By analyzing the structures, we found that (HS)G/MoS_2 is more compact than impurity defected Nb-(HS)G/MoS_2 and Tc-(HS)G/MoS_2 materials. From the band structure calculations, we found that all the materials have metallic properties. It is found that n-type Schottky contact is formed in pristine (HS)G/MoS_2 and Tc impurity defect Tc-(HS)G/MoS_2 materials, and p-type Shottky contact is formed in Nb impurity defect Nb-(HS)G/MoS_2 material. Therefore, n-type Schottky contact of (HS)G/MoS_2 changes to p-type Schottky contact due to Nb impurity defect in (HS)G/MoS_2 material. To investigate the magnetic properties, we have carried out DoS and PDoS calculations, and found that (HS)G/MoS_2 is non-magnetic material, while Nb-(HS)G/MoS_2 and Tc-(HS)G/MoS_2 are magnetic materials. The total magnetic moment of Nb-(HS)G/MoS_2 and Tc-(HS)G/MoS_2 have values -0.24μ_B/cell and 0.07 μ_B/cell respectively. High value of magnetic moment is given by distributed unpaired up-spin and down-spin of electrons in 4p & 4d orbitals of Mo atoms; 3p orbital of S atoms in Nb-(HS)G/MoS_2 material, and 4d orbital of Mo atoms; 3p orbital of S atoms in Tc-(HS)G/MoS_2 material.

ACKNOWLEDGEMENTS

HK Neupane and NP Adhikari acknowledge to UGC Nepal, PhD grants of award no. PhD - 75/76 - S & T - 09, and UGC grants CRG 073/74 - S & T - 01 respectively. Also, NP Adhikari acknowledges to network project NT - 14 of ICTP/OEA.

REFERENCES

[1] Xu, M.; Liang, T.; Shi, M.; and Chen, H. Graphene-like two-dimensional materials. *Chemical Reviews*, **113**(5): 3766-3798 (2013).

[2] Mayorov, A. S.; Gorbachev, R. V.; Morozov, S. V.; Britnell, L.; Jalil, R.; Ponomarenko, L. A.; and Geim, A. K. Micrometer-scale ballistic transport in encapsulated graphene at room temperature. *Nano Letters*, **11**(6): 2396-2399 (2011).

[3] Morozov, S. V.; Novoselov, K. S.; Katsnelson, M. I.; Schedin, F.; Elias, D. C.; Jaszczak, J. A.; and Geim, A. K. Giant intrinsic carrier mobilities in graphene and its bilayer. *Physical Review Letters*, **100**(1): 016602 (2008).

[4] Novoselov, K. S.; Geim, A. K.; Morozov, S. V.; Jiang, D.; Katsnelson, M. I.; Grigorieva, I.; and Firsov, A. A. Two-dimensional gas of massless Dirac fermions in graphene. *Nature*, **438**(7065): 197-200 (2005).

[5] Lei, J. C.; Zhang, X.; and Zhou, Z. Recent advances in MXene: Preparation, properties, and applications. *Frontiers of Physics*, **10**(3): 276-286 (2015).

[6] Dávila, M. E.; Xian, L.; Cahangirov, S.; Rubio, A.; and Le Lay, G. Germanene: a novel two-dimensional germanium allotrope akin to graphene and silicene. *New Journal of Physics*, **16**(9): 095002 (2014).

[7] Balendhran, S.; Walia, S.; Nili, H.; Sriram, S.; and Bhaskaran, M. Elemental analogues of graphene: silicene, germanene, stanene, and phosphorene. *Small*, **11**(6): 640-652 (2015).

[8] Castro, E. V.; Novoselov, K. S.; Morozov, S. V.; Peres, N. M. R.; Dos Santos, J. L.; Nilsson, J.; and Neto, A. C. Biased bilayer graphene: semiconductor with a gap tunable by the electric field effect. *Physical Review Letters*, **99**(21): 216802 (2007).

[9] Mak, K. F.; Lee, C.; Hone, J.; Shan, J.; and Heinz, T. F. Atomically thin MoS_2: a new direct-gap semiconductor. *Physical Review Letters*, **105**(13): 136805 (2010).

[10] Kadantsev, E. S.; and Hawrylak, P. Electronic structure of a single MoS_2 monolayer. *Solid State Communications*, **152**(10): 909-913 (2012).

[11] Zhang, Y.; Ye, J.; Matsuhashi, Y.; and Iwasa, Y. Ambipolar MoS_2 thin flake transistors. *Nano Letters*, **12**(3): 1136-1140 (2012).

[12] Radisavljevic, B.; Whitwick, M. B.; and Kis, A. Small-signal amplifier based on single-layer MoS_2. *Applied Physics Letters*, **101**(4): 043103 (2012).

[13] Fornarini, L.; Stirpe, F.; Scrosati, B.; and Razzini, G. Electrochemical solar cells with layer-type semiconductor anodes. Performance of n-MoS2 cells. *Solar Energy Materials*, **5**(1): 107-114 (1981).

[14] Hu, K. H.; Hu, X. G.; Wang, J.; Xu, Y. F.; and Han, C. L. Tribological properties of MoS_2 with different morphologies in high-density

polyethylene. *Tribology Letters*, **47**(1): 79-90 (2012).

[15] Britnell, L.; Gorbachev, R. V.; Jalil, R.; Belle, B. D.; Schedin, F.; Mishchenko, A.; and Peres, N. M. R. Field-effect tunneling transistor based on vertical graphene heterostructures. *Science*, **335**(6071): 947-950 (2012).

[16] Dean, C. R.; Young, A. F.; Meric, I.; Lee, C.; Wang, L.; Sorgenfrei, S.; and Hone, J. Boron nitride substrates for high-quality graphene electronics. *Nature Nanotechnology*, **5**(10): 722-726 (2010).

[17] Zhong, X.; Yap, Y. K.; Pandey, R.; and Karna, S. P. First-principles study of strain-induced modulation of energy gaps of graphene/BN and BN bilayers. *Physical Review B*, **83**(19): 193403 (2011).

[18] Debbichi, L.; Eriksson, O.; and Lebègue, S. Electronic structure of two-dimensional transition metal dichalcogenide bilayers from ab initio theory. *Physical Review B*, **89**(20): 205311 (2014).

[19] Neupane, H. K.; and Adhikari, N. P. Structure, electronic and magnetic properties of 2D Graphene-Molybdenum diSulphide (G-MoS2) Heterostructure (HS) with vacancy defects at Mo sites. *Computational Condensed Matter*, e00489 (2020).

[20] Neupane, H. K.; and Adhikari, N. P. Tuning Structural, Electronic, and Magnetic Properties of C Sites Vacancy Defects in Graphene/MoS2 van der Waals Heterostructure Materials: A First-Principles Study. *Advances in Condensed MatterPhysics*, *2020* (2020).

[21] Neupane, H. K.; and Adhikari, N. P. First-principles study of structure, electronic, and magnetic properties of C sites vacancy defects in water adsorbed graphene/MoS 2 van der Waals heterostructures. *Journal of Molecular Modeling*, **27**(3): 1-12 (2021).

[22] Neupane, H. K.; and Adhikari, N. P. Structural, electronic and magnetic properties of S sites vacancy defects graphene/MoS2 van der Waals heterostructures: First-principles study. *International Journal of Computational Materials Science and Engineering*, 2150009 (2021).

[23] Kittel, C.; McEuen, P.; and McEuen, P. Introduction to solid state Physics. *New York: Wiley*, **8**: 140-303 (1996).

[24] Hohenberg, P.; and Kohn, W. Inhomogeneous electron gas. *Physical Review*, **136**(3B): B864 (1964).

[25] Grimme, S. Accurate description of van der Waals complexes by density Functional theory including empirical corrections. *Journal of Computational Chemistry*, **25**(12): 1463-1473 (2004).

[26] Giannozzi, P.; Baroni, S.; Bonini, N.; Calandra, M.; Car, R.; Cavazzoni, C.; and Dal Corso, A. QUANTUM ESPRESSO: modular and open-source software Project for quantum simulations of materials. *Journal of Physics: Condensed Matter*, **21**(39): 395502 (2009).

[27] Perdew, J. P.; Burke, K.; and Ernzerhof, M. Generalized gradient approximation made simple. *Physical review letters*, **77**(18): 3865 (1996).

[28] Pfrommer, B. G.; Côté, M.; Louie, S. G.; and Cohen, M. L. Relaxation of Crystals with the quasi-Newton method. *Journal of Computational Physics*, **131**(1): 233-240 (1997).

[29] Pack, J. D.; and Monkhorst, H. J. Special points for Brillouin-zone integrations a reply. *Physical Review B*, **16**(4): 1748 (1977).

[30] Marzari, N.; Vanderbilt, D.; De Vita, A.; and Payne, M. C. Thermal Contraction and disordering of the Al (110) surface. *Physical review Letters*, **82**(16): 3296 (1999).

[31] Vu, T. V.; Hieu, N. V.; Phuc, H. V.; Hieu, N. N.; Bui, H. D.; Idrees, M.; and Nguyen, C. V. Graphene/WSeTe van der Waals heterostructure: Controllable electronic properties and Schottky barrier via interlayer coupling and electric field. *Applied Surface Science*, **507**: 145036 (2020).

[32] Alam, Q.; Muhammad, S.; Idrees, M.; Hieu, N. V.; Binh, N. T.; Nguyen, C.; and Amin, B. First-principles study of the electronic structures and optical and photocatalytic performances of van der Waals heterostructures of SiS, P and SiC monolayers. *RSC Advances*, **11**(24): 14263-14268 (2021).

[33] Hou, Z.; Wang, X.; Ikeda, T.; Terakura, K.; Oshima, M.; Kakimoto, M. A.; and Miyata, S. Interplay between nitrogen dopants and native point defects in graphene. *Physical Review B*, **85**(16): 165439 (2012).

[34] Phuc, H. V.; Hieu, N. N.; Hoi, B. D.; Phuong, L. T.; and Nguyen, C. V. First principle study on the electronic properties and Schottky contact of graphene adsorbed on MoS_2 monolayer under applied out-plane strain. *Surface Science*, **668**: 23-28 (2018).

[35] Liu, B.; Wu, L. J.; Zhao, Y. Q.; Wang, L. Z.; and Cai, M. Q. First-principles Investigation of the Schottky contact for the two-dimensional MoS_2 and graphene heterostructure. *RSC advances*, **6**(65): 60271-60276 (2016).